PCCP

Accepted Manuscript

ROYAL SOCIETY OF CHEMISTRY

www.rsc.org/pccp

Two-dimensional potential energy surface for proton transfer in acetylacetone and its α-halo derivatives

Fatmeh Dolati,[a] Sayyed Faramarz Tayyari,*[a] Mohammad Vakili,[a] and Yan Alexander Wang*[b]

[a] *Chemistry Department, Ferdowsi University of Mashhad, Mashhad, Iran.*

[b] *Department of Chemistry, University of British Columbia, Vancouver, BC V6T 1Z1, Canada*

Abstract

A two-dimensional potential energy surface was utilized to treat the proton transfer in acetylacetone (AA) and its α-halo derivatives: α-fluoro- (FAA), α-chloro- (ClAA), and α-bromo-acetylacetone (BrAA). This potential energy function, which couples O−H stretching and in-plane bending vibrations, was acquired through *ab initio* calculations for a fixed skeleton geometry. The resulting potential energy surfaces were then used to calculate the proton tunneling frequencies and proton transfer barrier heights. The barrier heights (the energy difference between the saddle point and the minima) calculated at the MP2/6-31G(2d,p) level of theory for proton transfers in AA, FAA, ClAA, and BrAA are 7.2, 9.4, 6.3, and 5.9 kcal/mol, respectively. The theoretically predicted proton transfer barrier heights exhibit excellent linear correlations with geometrical, electronic structural, and topological parameters evaluated within the atoms-in-molecule (AIM) and natural bond orbital (NBO) analyses.

Keywords: Acetylacetone; α-Halo-acetylacetones; Potential energy surface; Proton tunneling frequency; Two-dimensional double-minimum potential.

1. Introduction

β-Diketones constitute a class of organic compounds that have at least one α-hydrogen atom enable them to undergo keto-enol tautomerization. The cis-enol forms of β-diketones (Fig. 1) are stabilized by intramolecular hydrogen bond (IHB), whose strength is further enhanced by π-electron delocalization in the chelated ring [1]. This effect was named by Gilli *et al.* [1] as resonance assisted hydrogen bond.

IHB is the main factor for the high content of the enols in most β-diketone samples. In the case of symmetric β-diketones (*i.e.*, $R_1 = R_2$, $R_4 = H$ or D in Fig. 1), there should be two possibilities for the IHB proton movement in the cis-enols. The IHB proton may be localized in the mid-point between the two O atoms (O1 and O5), with a symmetric single-minimum potential function (Fig. 1b), or being near one of the two O atoms, with a symmetric double-minimum potential function (Fig. 1a). The IHB proton transfer in the enol form of β-diketones has been extensively investigated from both experimental [2−21] and theoretical [22−34] points of view.

Among the two simplest members of this class of compounds, malonaldehyde ($R_1 = R_2 = R_3 = R_4 = H$ in Fig. 1) and acetylacetone ($R_1 = R_2 = CH_3$, $R_3 = R_4 = H$ in Fig. 1), acetylacetone (AA) offers more intriguing interplay between the IHB proton transfer and the conformations of the two terminal methyl groups. Take the ground state of the C_s conformation of AA (Fig. 1a) for example, the methyl group (R_1) on the O1−H6 side is in the gauche position with respect to the sp^3 O1 atom whereas the methyl group (R_2) on the C4=O5 side is in the eclipsed position with respect to the sp^2 O5 atom. During the H6 transfer through the IHB setup (Fig. 1b), these two methyl groups must simultaneously rotate into an identical eclipsed position through a C_{2v} structure (Fig. 1b) to achieve the minimum energy. Based on such an understanding, Rios and Rodríguez investigated the IHB proton transfer in AA and obtained a double minimum potential function with a barrier height of about 7 kcal/mol [22]. On the other hand, *ab initio* calculations performed by Matanović *et al.* concluded a barrier of only half the height, 3.4 kcal/mol, for the IHB proton transfer in AA [23]. Previous attempt to observe the tunneling frequency for AA in the gas, liquid, or solid state were not successful [9,10]. It becomes desirable to appreciate whether such a discrepancy can be attributed to an asymmetric structure due to different conformations of the two terminal methyl groups in the AA molecule during the IHB proton transfer.

The structure and the IHB of AA have been subjected to many theoretical [26−33] and experimental [9−23] investigations, but the most stable form between the C_{2v} and C_s structures (Fig. 1) still remain unresolved. An early electron diffraction (ED) [15] and a later microwave investigations [21] have identified the C_{2v} structure to be the dominate enol form of AA. However, many other investigations based on neutron [12] and X-ray crystallography [13,14], liquid NMR [19], gas phase ED [17,20], and vibrational spectroscopy [9−11] supported the C_s structure to be the dominate enol form of AA in the gas, liquid, and solid phases, in agreement with the results of almost all theoretical studies [26−33].

For the simpler malonaldehyde (MA) system, experimental [2−5] and theoretical studies [24] all established that the IHB proton transfer follows a symmetric double-minimum potential with a proton tunneling frequency of about 22 cm^{-1}. Tayyari *et al.* [24] applied two-dimensional symmetric double minimum potential for the hydrogen transfer in the bent IHB system and correctly obtained the proton tunneling frequencies of MA [24] and α-nitro-malonaldehyde (NO_2-MA) [25]. Such a model was also successfully applied to the IHB of 6-hydroxy-2-formylfulvene [34], a nearly linear hydrogen bonded system.

Based upon our previous success on the MA system, we aimed our investigation to the bent IHB system in AA and its α-halo derivatives by applying a similar two-dimensional potential surface for the IHB proton transfer processes. The obtained proton tunneling frequency and potential barrier height in AA were compared with those in α-fluoro (FAA), α-chloro (ClAA), and α-bromo (BrAA) derivatives to shed light on the nature of the IHB and to resolve any inconsistent results previously reported for such systems. The nature of IHBs in these systems was further examined within natural bond orbital (NBO) and atoms-in-molecules (AIM) analyses.

2. Computational Procedure

All *ab initio* calculations in this work were performed using the Gaussian 09W Package [35]. Since MP2 [36,37] was already demonstrated to produce superior theoretical results [24], we have thus employed it again for this study. However, the 6-31G(d,p) basis set, which was employed in previous work, is not capable of modeling the IHB of the BrAA system involving the Br atom (more on this in Section 3.1 below). The geometry optimizations were thus performed at the MP2 level of theory using two larger basis sets, 6-31G(2d,p) and 6-31G(df,p),

with two different enhanced polarization schemes instead. To evaluate the validity of theoretical results, similar calculations were also performed on MA and NO_2-MA for comparison purpose.

To explore the two-dimensional proton transfer potential surface, the O1−H6 distance in AA and its α-halo derivatives was varied from 0.90 to 1.18 Å (in steps of 0.01 Å) and the ∠O1−H6···O5 angle was scanned from 0° to 28° (in steps of 2°); the corresponding energies were calculated with all other geometrical parameters fixed at their optimized equilibrium values of the ground state. More specifically, to estimate the energy difference between the gauche and eclipsed conformations during proton movement, the ∠O1−H6···O5 angle was subsequently optimized while the O1−H6 distance was increased from 0.90 to 1.30 Å (in steps of 0.05 Å) with all other structural parameters frozen at their equilibrium positions. This scan gives the minimum potential energy in the two-dimensional (constrained) potential surface along the path from the minima to the saddle point. Such a scheme has been successfully applied before for a wide range of IHB systems with excellent agreement with experimental results [24,25,34].

The calculated potential energy surfaces were then fitted to the following anharmonic two-dimensional potential function:

$$V = \frac{1}{2}(K_s X^2 + K_{ss} X^4 + K_b Y^2 + K_{ssb} X^2 Y) \ , \quad (1)$$

where K_s and K_{ss} represent the quadratic and quartic force constants in the X (stretching) direction, respectively, K_b represents the quadratic force constant in the Y (bending) direction, and K_{ssb} represents the interaction between stretching and bending modes. The saddle point (*i.e.*, the transition state) of the IHB proton transfer process happens at $X = Y = 0$ and $V = 0$. The energies up to 2500 cm^{-1} from the bottom of potential wells (the minimum positions) were included in calculations.

The barrier heights were calculated as follows. At the minimum positions of the IHB proton transfer process, X_m and Y_m, we have

$$\frac{\partial V}{\partial X} = 0 = K_s X_m + 2K_{ss} X_m^3 + K_{ssb} X_m Y_m \quad (2)$$

and

$$\frac{\partial V}{\partial Y} = 0 = K_b Y_m + \frac{1}{2} K_{ssb} X_m^2 \ , \quad (3)$$

which immediately yield

$$X_m^2 = -2K_b Y_m / K_{ssb} \quad (4)$$

and

$$Y_m = K_s K_{ssb}/(4K_{ss}K_b - K_{ssb}^2) \ . \quad (5)$$

Consequently, the barrier height (the energy difference between the saddle point and the minima), E_{BH}, can be calculated readily,

$$E_{\mathrm{BH}} = -\frac{1}{2}(K_s X_m^2 + K_{ss} X_m^4 + K_b Y_m^2 + K_{ssb} X_m^2 Y_m) \ . \quad (6)$$

Concurrently, the barrier height measured at the midpoint between the two oxygen atoms (O1 and O5) from the minima, E'_{BH}, is slightly higher than E_{BH} by the amount of $\frac{1}{2}K_b Y_m^2$,

$$E'_{\mathrm{BH}} = -\frac{1}{2}(K_s X_m^2 + K_{ss} X_m^4 + K_{ssb} X_m^2 Y_m) \ . \quad (7)$$

Physically, E'_{BH} is the barrier height between the two minima if the O1−H6···O5 system is a linear IHB (*i.e.*, tunneling occurs directly between the two minima). In reality, though, the effective barrier height lies somewhere between E_{BH} and E'_{BH}.

For the purpose of brevity, the readers are directed to our previously publications [24,25,34] for a full explanation on the detailed procedure of obtaining the energy levels and tunneling frequencies.

The nature of the IHBs within AA and its α-halo derivatives can also been studied with the AIM theory [38], because the electronic density at the bond critical point (CP), $\rho_c(\mathbf{r})$, and its Laplacian, $\nabla^2\rho_c(\mathbf{r})$, are useful parameters for the estimation of the relative strength of hydrogen bonding [39]. According to Espinosa and Molins [40], hydrogen bond strength (E_{HB}), is equal to one-half of the local potential energy density $V_\rho(\mathbf{r})$ at the hydrogen bond CP:

$$E_{\mathrm{HB}} = -\frac{1}{2}V_\rho(\mathbf{r}) \ . \quad (8)$$

3. Results and Discussion

3.1. Potential Surfaces

Among the theoretical results of selected potential energy surface and structural parameters, proton transfer barrier heights, and proton tunneling frequencies depicted in Table 1, the magnitudes of the proton transfer barrier heights, E_{BH} and E'_{BH}, directly signify the strength of the IHB: the lower the proton transfer barriers, the easier the proton transfer, and thus the stronger the IHB.

First, the positive values of E_{BH} and E'_{BH} clearly verify that the C_s structure (Fig. 1a) is the ground state for AA and its α-halo derivatives, consistent to nearly all previous experimental and theoretical conclusions [9−14,17,19,20,26−33], except for only two experiments [15,21].

Second, calculations with the 6-31G(d,p) basis set predicted a weaker IHB in BrAA than in ClAA, which is opposite to the results with the 6-31G(2d,p) and 6-31G(df,p) basis sets. In a well-established NMR experiment [41], the chemical shifts of the enolated proton in ClAA and BrAA were observed at 15.35 and 15.75 ppm, respectively, suggesting the IHB in BrAA to be considerably stronger than that in ClAA. We thus conclude that the 6-31G(d,p) basis set has some deficiency in modeling the BrAA and ClAA systems.

On the other hand, calculations with the two other better basis sets, 6-31G(2d,p) and 6-31G(df,p), produced very similar results for the proton transfer barrier heights and proton tunneling frequencies (see Table 1). This demonstates that a higher level of polarization in the Pople's basis set, *e.g.*, (2d,p) and (df,p), is critical for generating reliable results but offers very little difference once the basis-set enhancement in polarization goes beyond the (d,p) level.

Furthermore, we can rely on the experimental data to gauge the quality of our theoretical results. For MA and its deuterated analogous D_2MA (R3=R4=D in Fig. 1), the observed proton tunneling frequencies of the benchmark systems are 21.58 and 2.88 cm^{-1} [5], respectively. The corresponding values for NO_2-MA and its deuterayed analogue are 35 ± 15 and 3.00 ± 0.02 cm^{-1} [7], respectively. In all such cases, our theoretical predictions agree very well with the available experimental data [5,7], although the computational results based on the 6-31G(2d,p) basis set are slightly better than those of the 6-31G(df,p) basis set. Thereby, we will proceed forthcoming discussions mainly based upon the MP2/6-31G(2d,p) results (especially in the presentation of Figs. 2−4).

According to our calculations with the 6-31G(2d,p) basis set, the predicted proton transfer barrier heights, E_{BH}, for AA, BrAA, ClAA, FAA, NO_2-MA, and MA are about 7.2, 5.9, 6.3, 9.4, 7.7, and 8.7 kcal/mol, respectively. The proton tunneling frequencies for AA and its partially deuterated partner, D_2AA, are estimated to be around 65 and 8 cm^{-1}, respectively. In comparison, our calculated barrier height for AA is in excellent agreement with that predicated by Rios and Rodríguez [22], but is twice the magnitude of that by Matanović *et al*. [23]. Given that our modeling yields highly consistent results to previous extensive experimental and theoretical studies on MA and its derivatives [5,7,24,25], we thus have confidence in our theoretically predicted IHB proton transfer barrier heights for AA and D_2AA.

Naturally, one might envision that the transition state of the IHB proton transfer process resembles the C_{2v} structure shown in Fig. 1b. We hence searched for such a C_{2v} transition state for MA and D_2MA with all other geometrical parameters fully relaxed. Eventually, we indeed identified the C_{2v} "transition state" but unfortunately with much lower barrier heights: $E_{BH} = 3.7$ kcal/mol and $E'_{BH} = 6.1$ kcal/mol, very similar to the situation in AA encountered by Matanović *et al*. previously [23]. Moreover, with such small barriers, the proton tunneling frequencies for MA and D_2MA were predicted to be over 120 and 25 cm^{-1}, respectively, nearly 6 and 9 times bigger than the experimental values, 21.58 and 2.88 cm^{-1} [5]. Obviously, the IHB proton tunneling is an early, sudden *quantum* process without going through the *classical* C_{2v} transition state. Such an understanding lends strong support to our two-dimensional potential energy surface model for the IHB proton transfer process, in which we only scanned the O1−H6 distance and the ∠O1−H6···O5 angle and kept all other geometrical parameters fixed at their optimized equilibrium values.

3.2. Structural Parameters

Selected structural parameters intimately related to the IHBs of AA, FAA, ClAA, BrAA, MA, and NO_2-MA are also collected in Table 1. Our theoretical results with both basis sets clearly show that the O1···O5 and O5···H6 distances follow the trend: FAA > MA > NO_2-MA > AA > ClAA > BrAA, exactly in an inverse correlation with the O1−H6 distance and the IHB strength as being consistently predicted by the proton transfer barrier heights, E_{BH} and E'_{BH}.

In comparison with MA, the two methyl groups in AA exert extra steric and electron-donating effects that strengthen the IHB in AA. Likewise, in ClAA and BrAA, the repulsion between the H atoms of the methyl groups and the lone pairs of electrons in the halogen atoms in turn increases the steric tension between the two methyl groups and the lone pairs of electrons on the O1 and O5 atoms. As a result, both ClAA and BrAA possess stronger IHB than AA does.

To investigate the influence of the relative conformations of the two terminal methyl groups in AA on its IHB proton transfer process, we rotated both methyl groups into either staggered or eclipsed orientation to both O1 and O5 atoms. For these two conformations, we subsequently scanned the O1−H6 distance from 0.90 to 1.30 Å (to reach the C_{2v} transition state) and optimized the corresponding ∠O1−H6···O5 angle (among all structural parameters). From their energies (measured from the asymmetric ground state) plotted in Fig. 2a, we immediately

found that for all points leading to the C_{2v} transition state, any rotation of the two terminal methyl groups away from the asymmetric ground state must pay a penalty of higher energy.

More specifically, simultaneously staggered methyl groups agitate the electron structure much more than concurrently eclipsed methyl groups do. As the system approaches the C_{2v} transition state, the energy differences are smoothly shrinking to zero. Only at the C_{2v} transition state, the energy gaps between all different conformations of the two terminal methyl groups vanish completely: the methyl groups can rotate freely. In combination with Section 3.2, we therefore can draw a convincing conclusion that our two-dimensional potential energy surface, despite for its simplicity, is adequate in modeling the IHB proton tunneling process even without incorporating the rotations of the two terminal methyl groups in the formulation explicitly.

Figures 2b−2d exhibit excellent linear correlations between the IHB proton transfer barrier heights, E_{BH} and E'_{BH}, and the essential geometrical parameters of the IHB systems, the O1···O5, O5···H6, and O1−H6 distances. Such results suggest that the proton transfer barrier heights, E_{BH} and E'_{BH}, can be utilized for the characterization of the bent IHB systems, at least for the six molecules studied herein.

Additionally, the linear correlations shown in Fig. 2b predict that the proton transfer barrier will disappear when $R_{O1\cdots O5}$ contracts to 2.38 Å, which corresponds to a hydrogen bond strength $E_{HB} \approx 28$ kcal/mol (see Section 3.4 for more details on E_{HB}). Consistent results can also be derived from the linear correlations of E_{HB} with $R_{O5\cdots H6}$ (Fig. 2c) and with R_{O1-H6} (Fig. 2d).

3.3. NBO Analysis

The Wiberg bond orders [42] of the O1−H6, O5···H6, and O1···O5 atom pairs and the natural charges on the H6, O1, and O5 three atoms predominantly involved in the IHB for AA and its derivatives are gathered in Table 2. Not surprisingly, the trend of the predicted proton transfer barrier heights (thus the opposite trend of the IHB strength) indeed correlate positively with the O1−H6 bond order (Fig. 3a) and negatively with the O5···H6 bond order (Fig. 3b). These results are consistent with the theoretical results discussed in Sections 3.1 and 3.2.

Qualitatively, we expect that an increased IHB strength should enlarge the partial charge on O1, reduce the partial charges on O5 and H6, and raise the O1···O5 bond order. However, our theoretical results assembled in Table 2 reveal that the O1···O5 bond order and charges on O1, O5, and H6 are much less successful in quantifying the relative order of the IHB strength among the six molecules investigated here. Compared with the excellent correlations between the proton

transfer barrier heights, E_{BH} and E'_{BH}, and the O1−H6 (Fig. 3a) and O5···H6 (Fig. 3b) bond orders, there exists a very weak correlation between the barrier heights and the natural charge on the enol proton H6, Q_{H6} (Fig. 3c). However, if the Q_{H6} data points of FAA and NO_2-MA are excluded from the linear fitting, the quality of the correlation between the barrier heights and Q_{H6} becomes greatly improved (Fig. 3d). Evidently, the extremely electronegative F atom in FAA and NO_2 group in NO_2-MA abnormally withdraw too much electron cloud from the H6 atom and diminish the usefulness of utilizing Q_{H6} to ascertain the relative strength of the IHBs.

3.4. AIM Analysis

To further assess the IHB character, the topology of the electron density calculated at the MP2/6-31G(2d,p) and MP2/6-31G(df,p) levels of theory was diagnosed within the atoms-in-molecules (AIM) analysis [40]. According to the AIM theory, the structural elements constituted a molecule are identified at the critical points of the electron density distribution, $\rho_c(\mathbf{r})$: atoms corresponding to local maxima, bonds and rings to saddle points, and cages to local minima. The sign of the Laplacian, ∇^2, of the electron density at a bond critical point implies whether the charge is concentrated, as in covalent bonds $\nabla^2\rho_c(\mathbf{r}) < 0$, or depleted, as in ionic and hydrogen bonds $\nabla^2\rho_c(\mathbf{r}) > 0$. Thus, the AIM theory provides another analytical tool for describing the nature of the IHBs in AA and its derivatives.

At the hydrogen bond critical point, the calculated total electronic density, $\rho_c(\mathbf{r})$, the corresponding Laplacian, $\nabla^2\rho_c(\mathbf{r})$, the hydrogen bond strength, E_{HB}, the (negative) potential electron energy density, $-V_\rho(\mathbf{r})$, the kinetic electron energy density, $G_\rho(\mathbf{r})$, and their ratio (GVR), $-G_\rho(\mathbf{r})/V_\rho(\mathbf{r})$, are displayed in Table 3. It is illuminating to know that for all six molecules studied in this work, their GVR values at the hydrogen bond critical points are less than one, unveiling a partially covalent character of the IHBs [43].

Also, in agreement with the above discussions in Sections 3.1−3.3, E_{HB} estimated within the AIM analysis does indeed manifest strong linear correlations with the key geometrical parameters (*i.e.*, $R_{O1\cdots O5}$, $R_{O5\cdots H6}$, and R_{O1-H6}) and the proton transfer barrier heights (*i.e.*, E_{BH} and E'_{BH}) of the IHB systems (Fig. 2).

Given the fact that the proton transfer barrier heights, E_{BH} and E'_{BH}, possess excellent linear correlations with E_{HB} (Fig. 2) and the AIM topological parameters (Fig. 4), $\rho_c(\mathbf{r})$ and $\nabla^2\rho_c(\mathbf{r})$, we therefore conclude that E_{BH} and E'_{BH} are accurate indicators of hydrogen bond strength for symmetric resonance assisted hydrogen bond systems.

4. Conclusion

The geometries of AA, its α-halo derivatives, MA and NO_2-MA were optimized at the MP2 level of theory with 6-31G(df,p) and 6-31G(2d,p) basis sets. Based on these calculations, two-dimensional symmetric double minimum potential energy surfaces were obtained for the bent IHB systems of the six molecules. The proton transfer barrier heights, E_{BH} and E'_{BH}, of these IHB systems were predicted to be within the ranges of 5.6−9.4 and 7.6−12.8 kcal/mol, respectively. The proton transfer barrier heights, E_{BH} and E'_{BH}, demonstrate excellent linear correlations with geometrical and AIM topological parameters. Computational results confirm that E_{BH} and E'_{BH} are effective descriptors for the IHBs within the symmetric hydrogen bonded systems.

Acknowledgements

Y.A.W. thanks the Natural Sciences and Engineering Research Council (NSERC) of Canada for financial support. The authors would like to thank Ms. Mansoureh Keikhaei for her help in drawing the potential surface diagrams.

References

1. G. Gilli, F. Belluci, V. Ferretti, V. Bertolesi, *J. Am. Chem. Soc.***1989**, *111*, 1023–1028.
2. W. F. Rowe, R. W. Duerst, E. B. Wilson, *J. Am. Chem. Soc*. **1976**, *98*, 4021.
3. S. L. Baughcum, R. W. Duerst, W. F. Rowe, Z. Smith, E. B. Wilson, *J. Am. Chem. Soc*. **1981**, *103*, 6296.
4. S. L. Baughcum, Z. Smith, E. B. Wilson, R. W. Duerst, *J. Am. Chem. Soc*. **1984**, *106*, 2260.
5. P. Turner, S. L. Baughcum, S. L. Coy, Z. Smith, *J. Am. Chem. Soc*. **1984**, *106*, 2265.
6. N. D. Sanders, *J. Mol. Spectrosc*. **1981**, *86*, 27.
7. W. Caminati, *J. Chem. Soc., Faraday Trans. 2* **1982**, *78*, 825.
8. S. F. Tayyari, F. Milani-Nejad, *Spectrochim. Acta Part A* **1998**, *54*, 255.
9. S. F. Tayyari, T. Zeegers-Huyskens, J. L. Wood, *Spectrochim. Acta Part A* **1979**, *35*, 1289.
10. S. F. Tayyari, Ph.D. Thesis, London University, 1978.
11. S. F. Tayyari, F. Milani-Nejad, *Spectrochim. Acta Part A* **1998**, *56*, 2679.
12. M. R. Johnson, N. H. Jones, A. Geis, A. J. Horsewill, H. P. Trommsdorff, *J. Chem. Phys*. **2002**, *116*, 5694.
13. A. Camerman, D. Mastropaolo, N. Camerman, *J. Am. Chem. Soc*. **1983**, *105*, 1584.
14. R. Boese, M. Y. Antipin, D. Bläser, K. A. Lyssenko, *J. Phys.Chem. B* **1998**, *102*, 8654.
15. A. H. Lowrey, C. George, P. D'Antonio, J. Karle, *J. Am. Chem. Soc*. **1971**, *93*, 6399.
16. A. L. Andreassen, S. H. Bauer, *J. Mol. Struct*. **1972**, *12*, 381.
17. K. Iijima, A. Ohnogi, S. Shibata, *J. Mol. Struct*. **1987**, *156*, 111.
18. R. K. Harris, R. C. Rao, *Org. Magn. Reson*. **1983**, *21*, 580.
19. W. Egan, G. Gunnarsson, T. E. Bull, S. Forsen, *J. Am. Chem. Soc.* **1977**, *99*, 4568.
20. R. Srinivasa, J. S. Feenstra, S. T. Park, S. Xu, A. H. Zewail, *J. Am. Chem. Soc*. **2004**, *126*, 2266.
21. W. Caminati, J.-U. Grabow, *J. Am. Chem. Soc*. **2006**, *128,* 854.
22. M. A. Rios, J. Rodríguez, *J. Mol. Struct.(Theochem)* **1990**, *204*, 137.
23. I. Matanović, N. Došlić, Z. Mihalić, *Chem. Phys.* **2004**, *306*, 201.
24. S. F. Tayyari, M. Zahedi, F. Tayyari, F. Milani-Nejad, *J. Mol. Struct. (Theochem)* **2003**, *637*, 171.
25. S. F. Tayyari, M. Zahedi-Tabrizi, H. Azizi-Toopkanloo, S. S. Hepperle, Y. A. Wang, *Chem. Phys.* **2010**, *368,* 62.
26. N. S. Hush, M. K. Livett, J. B. Peel, G. D. Willett, *Aust. J. Chem*. **1987**, *40*, 599.

27. J. J. Dannenberg, R. Rios, *J. Phys. Chem.* **1994**, *98*, 6714.
28. T. Ishida, F. Hirata, S. Kato, *J. Chem. Phys.* **1999**, *110*, 3938.
29. S. H. Bauer, C. F. Wilcox, *Chem. Phys. Lett.* **1997**, *279*, 122.
30. O. A. Sharafeddin, K. Hinsen, T. Carrington Jr., B. Roux, *J. Comput. Chem.* **1997**, *18*, 1760.
31. J. Mavri, J. Grdadolnik, *J. Phys. Chem. A* **2001**, *105*, 2039.
32. S. J. Grabowski, *J. Phys. Org. Chem.* **2003**, *16*, 797.
33. V. B. Delchev, H. Mikosch, G. S. Nikolov, *Monatsh. Chem.* **2001**, *132*, 339.
34. S. F. Tayyari, M. Zahedi-Tabrizi, H. Rahemi, H. A. Mirshahi, J. S. Emampour, M. Rajabi, F. Milani-Nejad, *J. Mol. Struct. (Theochem)* **2005**, *730*, 17-21.
35. Gaussian 09, Revision A.02, M. J. Frisch, G. W. Trucks, H. B. Schlegel, G. E. Scuseria, M. A. Robb, J. R. Cheeseman, G. Scalmani, V. Barone, B. Mennucci, G. A. Petersson, H. Nakatsuji, M. Caricato, X. Li, H. P. Hratchian, A. F. Izmaylov, J. Bloino, G. Zheng, J. L. Sonnenberg, M. Hada, M. Ehara, K. Toyota, R. Fukuda, J. Hasegawa, M. Ishida, T. Nakajima, Y. Honda, O. Kitao, H. Nakai, T. Vreven, J. A. Montgomery, Jr., J. E. Peralta, F. Ogliaro, M. Bearpark, J. J. Heyd, E. Brothers, K. N. Kudin, V. N. Staroverov, R. Kobayashi, J. Normand, K. Raghavachari, A. Rendell, J. C. Burant, S. S. Iyengar, J. Tomasi, M. Cossi, N. Rega, J. M. Millam, M. Klene, J. E. Knox, J. B. Cross, V. Bakken, C. Adamo, J. Jaramillo, R. Gomperts, R. E. Stratmann, O. Yazyev, A. J. Austin, R. Cammi, C. Pomelli, J. W. Ochterski, R. L. Martin, K. Morokuma, V. G. Zakrzewski, G. A. Voth, P. Salvador, J. J. Dannenberg, S. Dapprich, A. D. Daniels, O. Farkas, J. B. Foresman, J. V. Ortiz, J. Cioslowski, D. J. Fox, Gaussian, Inc., Wallingford CT, 2009.
36. A. D. Becke, *J. Chem. Phys.* **1993**, *98,* 5648.
37. C. Lee, W. Yang, R. G. Parr, *Phys. Rev. B* **1988**, *37*, 785.
38. R. F. W. Bader, Atoms in Molecules. A Quantum Theory, Oxford University Press, New York, 1990.
39. E. Espinosa, M. Souhassou, H. Lachekar, C. Lecomte, *Acta Crystallogr. B*, **1999**, *55*, 563 (and references cited therein).
40. E. Espinosa, E. Molins, *J. Chem. Phys.* **2000**, *113*, 5686.
41. J. L. Burdett, M. T. Rogers, *J. Am. Chem. Soc.* **1964**, *86*, 2105.
42. K. W. Wiberg, *Tetrahedron*. **1968**, *24,* 1083.
43. B. A. Shainyan, N. N. Chipanina, T. N. Aksamentova, L. P. Oznobikhina, G. N. Rosentsveig, I. B. Rosentsveig, *Tetrahedron* **2010**, *66*, 8551.

Figure Captions

Figure 1. Possible structures for cis-enol form of β-diketones and atom numbering system.

Figure 2. (**a**) Molecular energies of AA (with respect to its ground-state energies) with both methyl groups either eclipsed (green hollow squares) or staggered (red spheres) to the O1 and O5 atoms for an increasing O1−H6 distance from 0.90 to 1.30 Å. Linear correlations between E_{BH} (blue diamonds), E'_{BH} (brown squares), and E_{HB} (black triangles) and (**b**) O1···O5, (**c**) O5···H6, and (**d**) O1−H6 distances for the six molecules under investigation. All results are based on MP2/6-31G(2d,p) calculations.

Figure 3. Linear correlations between the proton transfer barrier heights, E_{BH} (diamonds) and E'_{BH} (squares), and (**a**) the O1−H6 bond order (W_{O1-H6}), (**b**) the O5···H6 bond order ($W_{O5\cdots H6}$), (**c**) the natural charge on the H6 atom (Q_{H6}), and (**d**) the natural charge on the H6 atom (Q_{H6}) excluding FAA (in red) and NO_2-MA (in red). All results are based on MP2/6-31G(2d,p) calculations.

Figure 4. Linear correlations between the proton transfer barrier heights, E_{BH} (blue diamonds) and E'_{BH} (brown squares), and (**a**) $\rho_c(\mathbf{r})$ and (**b**) $\nabla^2\rho_c(\mathbf{r})$. All results are based on MP2/6-31G(2d,p) calculations.

Table Captions

Table 1. Hydrogen bond structural parameters, proton transfer barrier heights, and proton tunneling frequencies with the 6-31G(2d,p) and 6-31G(df,p) basis sets.

Table 2. Wiberg bond orders (W) and natural charges (Q) for the electronic structure of the IHB involving the H6, O1 and O5 atoms with the 6-31G(2d,p) and 6-31G(df,p) basis sets.

Table 3. Calculated topological parameters at the hydrogen bond critical point within the AIM analysis with the 6-31G(2d,p) and 6-31G(df,p) basis sets.

Figure 1. Possible structures for cis-enol form of β-diketones and atom numbering system.

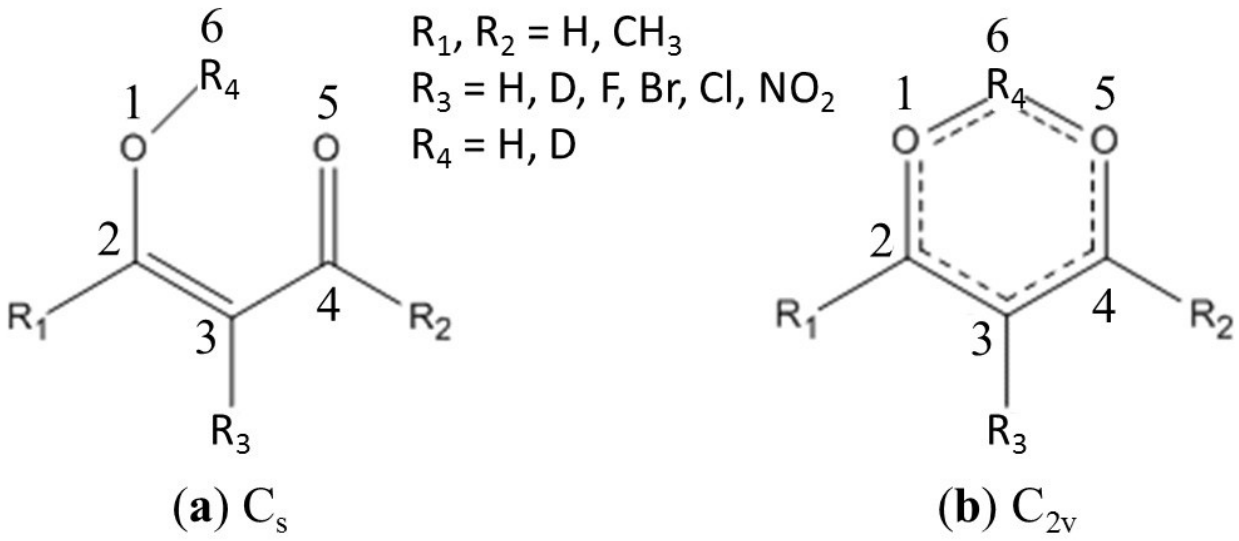

Figure 2. (**a**) Molecular energies of AA (with respect to its ground-state energies) with both methyl groups either eclipsed (green hollow squares) or staggered (red spheres) to the O1 and O5 atoms for an increasing O1−H6 distance from 0.90 to 1.30 Å. Linear correlations between E_{BH} (blue diamonds), E'_{BH} (brown squares), and E_{HB} (black triangles) and (**b**) O1···O5, (**c**) O5···H6, and (**d**) O1−H6 distances for the six molecules under investigation. All results are based on MP2/6-31G(2d,p) calculations.

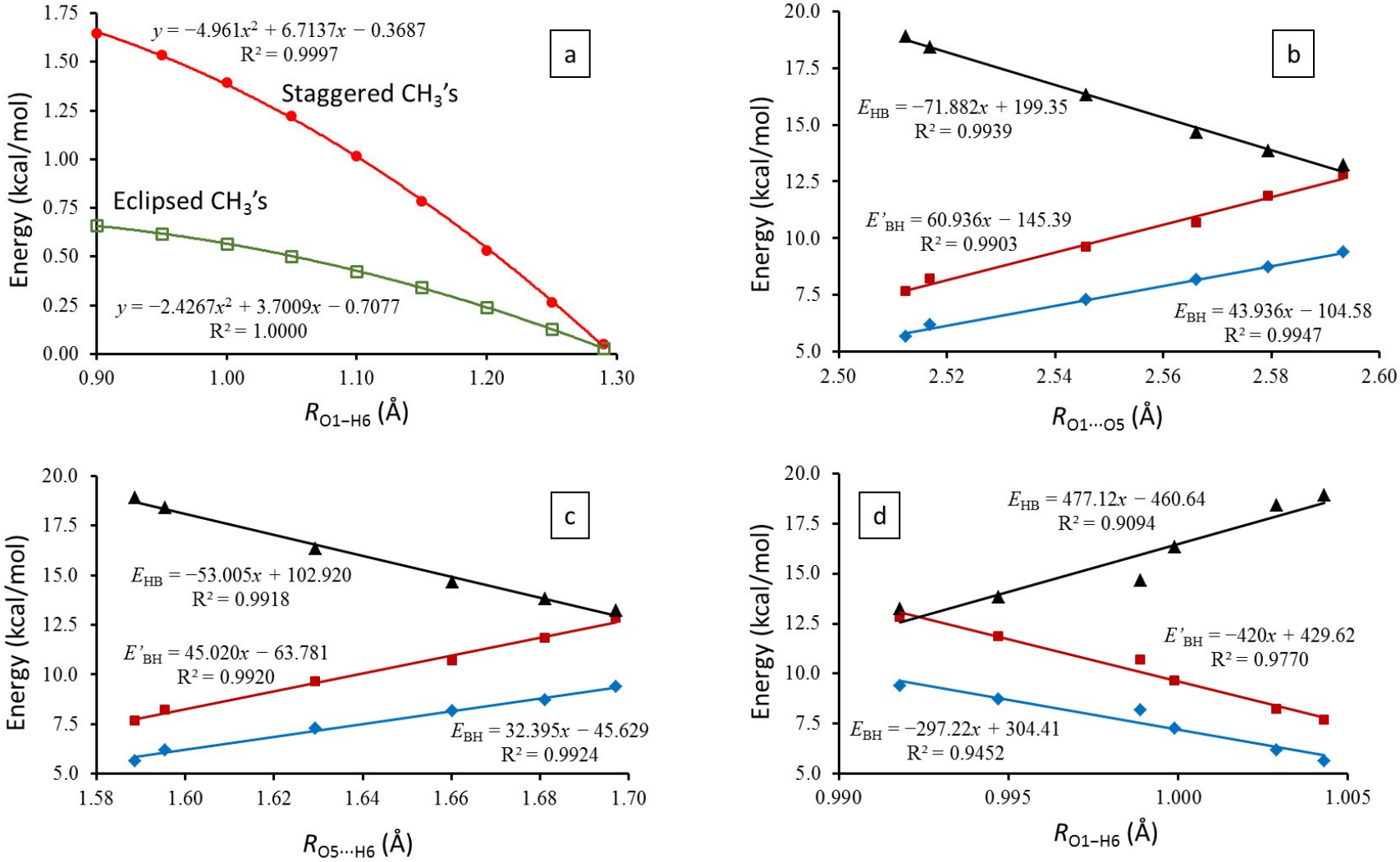

Figure 3. Linear correlations between the proton transfer barrier heights, E_{BH} (diamonds) and E'_{BH} (squares), and (**a**) the O1−H6 bond order (W_{O1-H6}), (**b**) the O5···H6 bond order ($W_{O5\cdots H6}$), (**c**) the natural charge on the H6 atom (Q_{H6}), and (**d**) the natural charge on the H6 atom (Q_{H6}) excluding FAA (in red) and NO_2-MA (in red). All results are based on MP2/6-31G(2d,p) calculations.

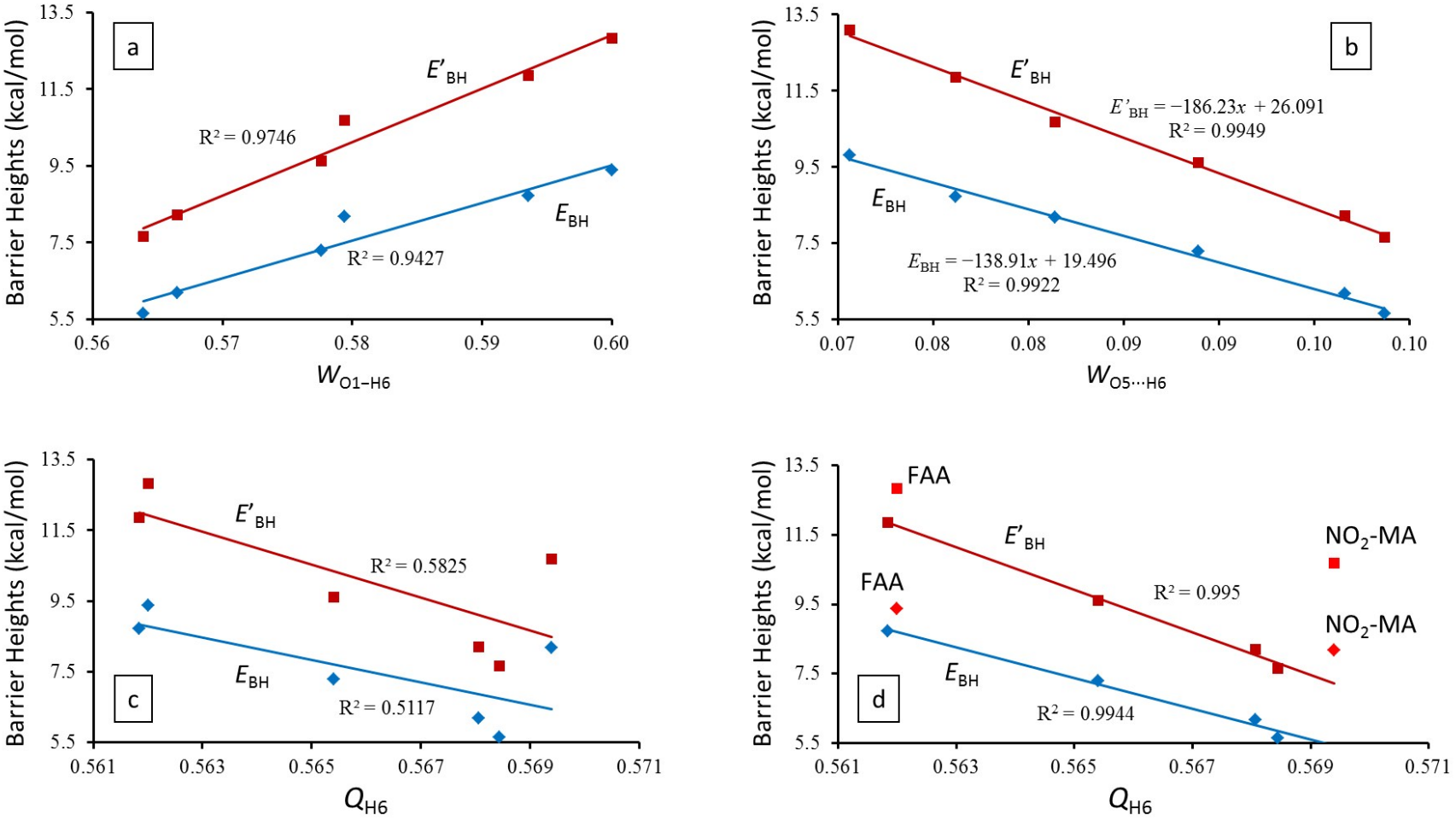

Figure 4. Linear correlations between the proton transfer barrier heights, E_{BH} (blue diamonds) and E'_{BH} (brown squares), and (**a**) $\rho_c(\mathbf{r})$ and (**b**) $\nabla^2\rho_c(\mathbf{r})$. All results are based on MP2/6-31G(2d,p) calculations.

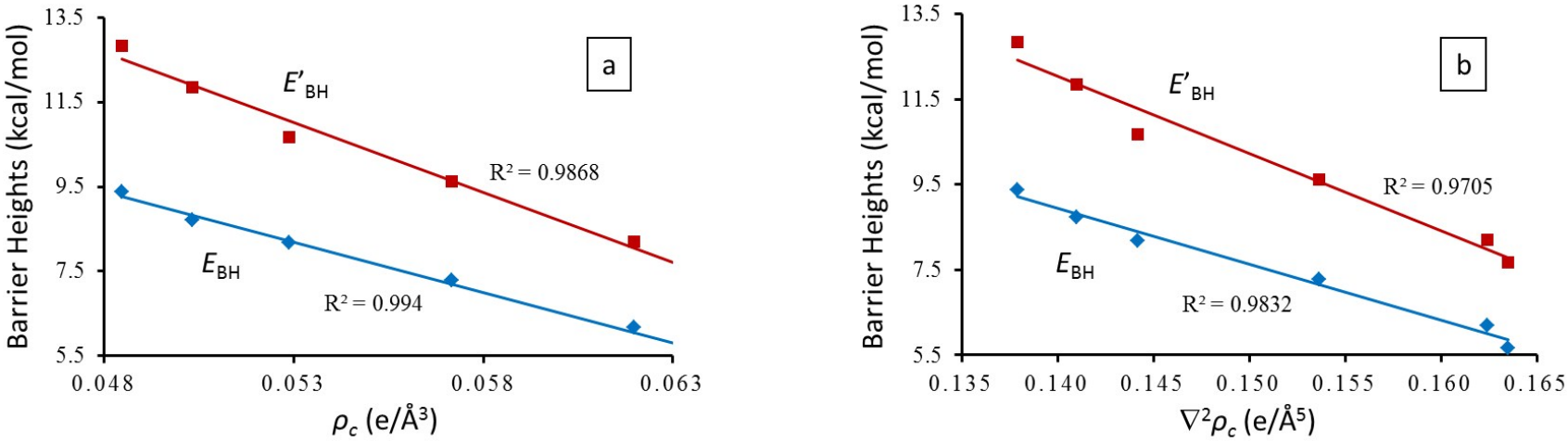

Table 1. Hydrogen bond structural parameters, proton transfer barrier heights, and proton tunneling frequencies with the 6-31G(2d,p) and 6-31G(df,p) basis sets [a]

Compound	$R_{O1\cdots O5}$ (Å)	R_{O1-H6} (Å)	$R_{O5\cdots H6}$ (Å)	∠O1−H6···O5 (degrees)	$\lvert X_m \rvert$ (Å)	Y_m (Å)	E_{BH} (kcal/mol)	E'_{BH} (kcal/mol)	ν_t [b] (cm^{-1})
6-31G(2d,p)									
BrAA	2.5261	1.0021	1.5958	150.8°	0.3127	0.1157	5.91	7.83	121/22
ClAA	2.5363	1.0008	1.6073	150.5°	0.3190	0.1190	6.27	8.31	101/16
AA	2.5586	0.9986	1.6342	150.5°	0.3335	0.1258	7.18	9.47	65/8.2
FAA	2.6108	0.9914	1.6914	148.9°	0.3673	0.1448	9.36	12.44	20/1.5
MA	2.5918	0.9948	1.6783	148.6°	0.3663	0.1462	8.67	11.78	25/2.0
NO_2-MA	2.5703	0.9988	1.6660	148.2°	0.3513	0.1325	7.73	10.33	40/4.0
6-31G(df,p)									
BrAA	2.5124	1.0043	1.5879	150.7°	0.3113	0.1177	5.65	7.66	131/24
ClAA	2.5169	1.0029	1.5954	150.4°	0.3130	0.1189	6.18	8.21	114/19
AA	2.5458	0.9999	1.6293	150.2°	0.3309	0.1276	7.28	9.62	66/8.4
FAA	2.5933	0.9915	1.6971	148.3°	0.3704	0.1556	9.38	12.83	19/1.3
MA	2.5794	0.9947	1.6812	148.1°	0.3600	0.1455	8.72	11.85	27/2.3
NO_2-MA	2.5661	0.9991	1.6603	147.7°	0.3482	0.1373	7.95	10.67	42/4.2

[a] E_{BH} and E'_{BH} are proton transfer barrier heights measured at the saddle point and at the midpoint of O1 and O5 atoms from the energy minima, respectively. X_m and Y_m are the minimum positions for the IHB proton transfer process on the potential energy surface.

[b] The first value of the tunneling splitting frequency is for the normal molecule (with all ^1H isotopes) and the second frequency is for its deuterated analogous ($R_3 = R_4 = D$ in Fig. 1).

Table 2. Wiberg bond orders (W) and natural charges (Q) for the electronic structure of the IHB involving the H6, O1 and O5 atoms with the 6-31G(2d,p) and 6-31G(df,p) basis sets.

Compound	$W_{O5\cdots H6}$	W_{O1-H6}	$W_{O1\cdots O5}$	Q_{O1}	Q_{O5}	Q_{H6}
6-31G(2d,p)						
BrAA	0.0945	0.5645	0.0328	−0.7307	−0.7628	0.5692
ClAA	0.0912	0.5684	0.0324	−0.7224	−0.7632	0.5687
AA	0.0857	0.5775	0.0303	−0.7312	−0.7794	0.5661
FAA	0.0698	0.5969	0.0287	−0.7124	−0.7702	0.5632
MA	0.0756	0.5914	0.0310	−0.7150	−0.7676	0.5628
NO_2-MA	0.0797	0.5784	0.0287	−0.6902	−0.7349	0.5700
6-31G(df,p)						
BrAA	0.0987	0.5639	0.0336	−0.7388	−0.7737	0.5684
ClAA	0.0966	0.5665	0.0334	−0.7380	−0.7738	0.5681
AA	0.0889	0.5776	0.0310	−0.7458	−0.7892	0.5654
FAA	0.0706	0.6003	0.0289	−0.7275	−0.7804	0.5620
MA	0.0762	0.5936	0.0311	−0.7239	−0.7735	0.5618
NO_2-MA	0.0814	0.5794	0.0289	−0.7003	−0.7408	0.5694

Table 3. Calculated topological parameters at the hydrogen bond critical point within the AIM analysis with the 6-31G(2d,p) and 6-31G(df,p) basis sets [a]

Compound	$\rho_c(\mathbf{r})$	$\nabla^2\rho_c(\mathbf{r})$	$G_\rho(\mathbf{r})$	$-V_\rho(\mathbf{r})$	GVR	E_{HB}
6-31G(2d,p)						
BrAA	0.0617	0.1713	0.0408	0.0450	0.867	18.31
ClAA	0.0601	0.1681	0.0396	0.0433	0.874	17.61
AA	0.0565	0.1594	0.0455	0.0513	0.889	16.08
FAA	0.0494	0.1434	0.0491	0.0561	0.914	13.58
MA	0.0509	0.1466	0.0506	0.0584	0.907	14.11
NO_2-MA	0.0524	0.1483	0.0417	0.0464	0.900	14.55
6-31G(df,p)						
BrAA	0.0632	0.1635	0.0506	0.0603	0.839	18.91
ClAA	0.0620	0.1624	0.0496	0.0587	0.846	18.40
AA	0.0572	0.1536	0.0452	0.0520	0.869	16.32
FAA	0.0485	0.1379	0.0383	0.0421	0.910	13.21
MA	0.0503	0.1410	0.0397	0.0441	0.900	13.83
NO_2-MA	0.0529	0.1442	0.0414	0.0467	0.886	14.65

[a] $\rho_c(\mathbf{r})$ in e/Å^5, $\nabla^2\rho_c(\mathbf{r})$ in e/Å^3, E_{HB} in kcal/mol.